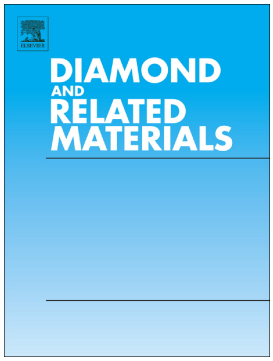

Thermal conductivity of free-standing CVD diamond films by growing on both nuclear and growth sides

Bing Dai, Jiwen Zhao, Victor Ralchenko, Andrey Khomich, Alexey Popovich, Kang Liu, Guoyang Shu, Ge Gao, Sun Mingqi, Lei Yang, Pei Lei, Jiecai Han, Jiaqi Zhu

PII: S0925-9635(16)30274-6
DOI: doi: 10.1016/j.diamond.2017.03.014
Reference: DIAMAT 6846

To appear in: *Diamond & Related Materials*

Received date: 30 June 2016
Revised date: 2 March 2017
Accepted date: 22 March 2017

Please cite this article as: Bing Dai, Jiwen Zhao, Victor Ralchenko, Andrey Khomich, Alexey Popovich, Kang Liu, Guoyang Shu, Ge Gao, Sun Mingqi, Lei Yang, Pei Lei, Jiecai Han, Jiaqi Zhu , Thermal conductivity of free-standing CVD diamond films by growing on both nuclear and growth sides. The address for the corresponding author was captured as affiliation for all authors. Please check if appropriate. Diamat(2017), doi: 10.1016/j.diamond.2017.03.014

Thermal conductivity of free-standing CVD diamond films by growing on both nuclear and growth sides

BingDai[a, #], Jiwen Zhao[a, #], Victor Ralchenko[a, c], Andrey Khomich[b, c], Alexey Popovich[b,c], Kang Liu[a], Guoyang Shu[a], Ge Gao[a], Sun Mingqi[a], Lei Yang[a], Pei Lei[a], Jiecai Han[a], Jiaqi Zhu[a,d,*]

[a]*Center for Composite Materials and Structures, Harbin Institute of Technology, Harbin, P. R. China*

[b]*Institute of Radio Engineering and Electronics RAS, Fryazino 141190, Russia*

[c] *General Physics Institute RAS, 38 Vavilov str., Moscow 119991, Russia*

[d]*Key Laboratory of Micro-systems and Micro-structures Manufacturing, Ministry of Education, Harbin 150080, P. R. China*

Abstract

Polycrystalline CVD diamond typically has inhomogeneous structure in cross section, with grain size monotonically increasing from bottom (nucleation) side to top (growth) side, this resulting in a significant difference in local thermal conductivity in the layers adjacent to the two surfaces. The polycrystalline diamond films with both sides of similar structure with coarse-grains are of interest for thermal management applications. Here, we produced a double-side coarse-grain polycrystalline diamond film by microwave plasma assisted chemical vapor deposition (MPCVD), by a repeated diamond growth on nucleation side of a primary free-standing film. The grain size, texture, morphology and phase purity of the samples were characterized with SEM, XRD and Raman spectroscopy, while the thermal conductivity (TC) perpendicularly to the film plane was measured by a laser flash technique in the temperature range of 250 – 400 K. The thermal conductivity of a single layer and bi-layered films are found to be almost identical, while the local TC values for latter on both sides are expected to become similar. A simple model discretizing the film in two regions, “poor” and “good” diamond layers, is considered to explain the observed TC temperature dependences.

Highlights

- Free-standing double-side grown diamond films are obtained by MPCVD.

-The film thermal conductivity (TC) is measured by a laser flash technique.

-The TC of the single layer (80 μm thick) and the bi-layer (160 μm) are found to be identical with 940 W/m·K.

- For all samples the TC shows a slight increasing trend with temperature in the range of 250 – 400K.

Keywords: microwave plasma CVD, polycrystalline diamond, thermal conductivity, laser flash technique

# These two authors contributed equally to this work.

Corresponding author, E-mail address: zhujq@hit.edu.cn (Jiaqi Zhu)

1. Introduction

Diamond possesses many extraordinary properties including very high thermal conductivity (TC). For single crystal diamond TC can reach 2200 W/m·K at room temperature [1], and similar local values were found for coarse-grained thick CVD diamond films [2], which is about 5 times more than that of copper (400 W/m·K) [3]. This property makes the CVD diamond a material of choice for heat spreaders in GaN LED [4], high electron mobility transistor GaN transistors [5], high power thin disk lasers [6], IR windows [7,8], and other applications which meet a critical problem of effective heat dissipation.

The polycrystalline CVD diamond films typically exhibit non-uniform structure with grain size increasing from the side adjacent to the substrate (nucleation) side to the top surface (growth side) as a result of competitive growth between differently oriented grains [9]. These structural features have a significant effect on thermal conductivity of the CVD diamond films, which appear to be non-uniform and anisotropic material in terms of thermal properties. First, the local thermal conductivity increases with the grain size due to a reduction in defects abundance and the number of grain boundaries in coarse-grain layers [10-12], therefore the TC increases from nucleation side to the growth one. In thin films with grain size of the order of 100 nm the TC is an order of magnitude lower compared to thicker films with grain size of tens microns [11]. Second, the in-plane ($k_{\parallel}$) TC and perpendicular ($k_{\perp}$) to the diamond surface thermal conductivities are different because of columnar structure of polycrystalline films. The columnar crystallites grow perpendicularly to the film surface, therefore phonons propagating along the column scatter with grain boundaries less frequently that those moving in-plane. The difference ($k_{\perp}>k_{\parallel}$) typically is of the order of 10% in thick diamond films [13], but in some cases it can be as high as 50% [14].

High quality polycrystalline CVD diamond (averaged over the thickness) shows TC for as high as 2000 W/(m·K) [13,15,16]. In thermal management, the heat dissipation of devices mounted on the nucleation side, can be essentially restricted

due to presence of small (submicron) grains, therefore, the heat source should be positioned preferably in proximity to the coarse-grain growth side. If the good TC required on both sides, a possible solution is the removal of the fine-grained defected layer on nucleation side by polishing or laser cutting to improve thermal conductivity of the substrate side and the average TC value [12]. Here, we report on an alternative way to eliminate the problem of low-TC material on one of the diamond film surfaces, and thus to increase local TC, but without removal of the nucleation layer. The approach is based on repeated growth of diamond on nucleation side of a free-standing diamond film to increase the film thickness and grain size on the (initially) nucleation side. In other words, the defective fine-grain layer is buried in the middle of the bi-layer film, which possesses now *two* growth sides. We produced diamond samples with large grains on both sides, and compared the thermal conductivity $k_{\perp}$ for single layer and double-layer films.

2. Experimental

The diamond films (see Table 1) were deposited on (100) oriented polished Si substrates (50 mm diameter, 1 mm thickness) in methane-hydrogen mixtures using a microwave plasma CVD system (PLASSYS SSDR150, 6 kW, 2.45 GHz). Prior the deposition the substrates were seeded by mechanical polishing with a diamond grit. The growth process was performed using total flow rate of 200 sccm, pressure of 168 mbar, microwave power of 3500W and the substrate temperature of 860°C as measured with a pyrometer (Williamson-92-40-C). First, the single layer diamond film #3 of ~80μm thickness was obtained after stable and continuous growth for 50h at relatively low CH_4 content (2%), then it was separated from the Si substrate by etching silicon in acid mixture of HNO_3 and HF. At the next step the growth was continued in the same regime on nucleation side of the sample #3 to prepare the double-layer sample #2 with total thickness doubled to 180 μm. The double-layer sample #1 was grown in a similar manner, with repeated growth on nucleation side to the total thickness of 180 μm in identical regimes, but at a higher CH_4 content (5%),

resulting in a more defective material. The double-layer sample #1 was opaque, whereas other two films #2 and #3 of better quality were translucent.

The free-standing films were characterized by secondary electron microscopy (SEM), X-ray diffraction (XRD) and Raman spectroscopy. The SEM images of the film surfaces and cross-sessions were obtained with Quanta 200 (FEI) instrument, and the film thickness was measured in cross-sections with the optical microscope OLS3100 (Olympus). Raman spectra, excited at 473 nm, were measured on both sides of each sample with a LabRam HR800 spectrometer (Horiba Jobin-Yvon) with spectral resolution of 1.0 cm^{-1} and spatial resolution of ~1 μm. The laser beam was focused on the sample surface, and the light from the sample has been collected in backscattering geometry with the microscope objective (Olympus, magnification ×100, numerical aperture NA = 0.90). The film texture was analyzed by XRD with a diffractometer (Empyrean, Panalytical) using Cu Kα radiation.

The thermal conductivity k in direction perpendicular to the film plane has been measured with the laser flash technique (LFT) as described elsewhere [17 - 19]. Briefly, the diamond film was mounted in the cryostat in a vacuum to minimize the convection heat dissipation. The thermal wave was generated on the front side of the sample by the laser pulses at wavelength λ=1.06 μm (pulse duration of 20 ns, energy 25 mJ, repetition rate of 1 Hz), while the temperature rise kinetics $T(t)$ on the rear side was traced by a fast HgCdTe infrared detector. The $T(t)$ curves exhibit a sharp rise front followed by a smooth approach to a plateau, with the typical time of temperature rise to ½ of temperature maximum being in the range of 2 - 18 μs depending on sample quality, thickness and temperature. The maximum rise ΔT of sample temperature at rear side of the sample caused by the laser heating was less than 2°C. The sample temperature was varied between 250 and 400K to measure k(T) dependence. To enhance the laser absorption and infrared emissivity a bi-layer Cu-Ti coating with thickness less than 300 nm was deposited on both sides of the sample. The kinetics $T(t)$ was averaged over 100 laser pulses to reduce the noise. The thermal diffusivity D was determined by fitting the experimental $T(t)$ curves to a modeled kinetics assuming one-dimensional heat flux [19]. Then, the thermal conductivity was

calculated as $k(T) = D(T)\rho C(T)$, where ρ = 3.51 g/cm^3 is mass density of diamond and $C(T)$ is specific heat of diamond as tabulated in [20]. The overall accuracy of the measurements was about ±15%. The LFT provides the TC value principally averaged over the sample thickness.

Table 1. Samples studied in this work: h is film thickness, Δν is the width (FWHM) of diamond Raman peak for two surfaces (surf 1 and surf 2), D is thermal diffusivity, k is thermal conductivity at room temperature measured by LFT.

Sample	color	h, μm	Δν, cm^{-1} surf 1/surf 2	D, cm^2/s	k, W/cm·K
#1 double	black	180	6.7/9.5	3.6	6.5±1.0
#2 double	white	160	2.2/2.8	5.2	9.4±1.4
#3 single	white	80	2.3/4.0	5.3	9.5±1.4

3. Results

3.1. SEM

The sample #3 (80 μm thick, single growth run) revealed crystallites with typical dimensions of 30-40 μm on growth side and of few microns on nucleation side (not shown here). The SEM images of the two growth surfaces for samples #1 and #2 are shown in Fig. 1. Hereafter, we define the following nomenclature for two surfaces of the samples produced by repeated growth, in other words, for the films having *two* growth surfaces, with nucleation side buried in between. The surface 1 is the growth surface of a single layer film after the 1st deposition run, while the surface 2 is the growth surface after the 2nd deposition run. Well-faceted grains with (111) dominant orientation, up to 50 μm in size, are seen for sample #2 (Fig. 1d, e). The grain size on the surface 2 is somewhat larger than for surface 1(~40 μm). This difference can be attributed to a change in diamond nucleation process on Si (sample #3), that proceeds on seeds, and on the substrate side of the primary diamond film upon the repeated growth, when the epitaxy occurs on continuous fine-grain surface. Many penetration twins can be seen on (111) facets on both sides, especially for opaque sample #1 (Fig.

1a, b), this being typical for (111) oriented films. The cross section (Fig. 1c, f) reveals a fine grained (nucleation) layer in the middle, the columnar crystallites extending in two directions, up and down. In contrast, the sample #1 demonstrates the grains of similar size on both sides (Fig. 1a, b).

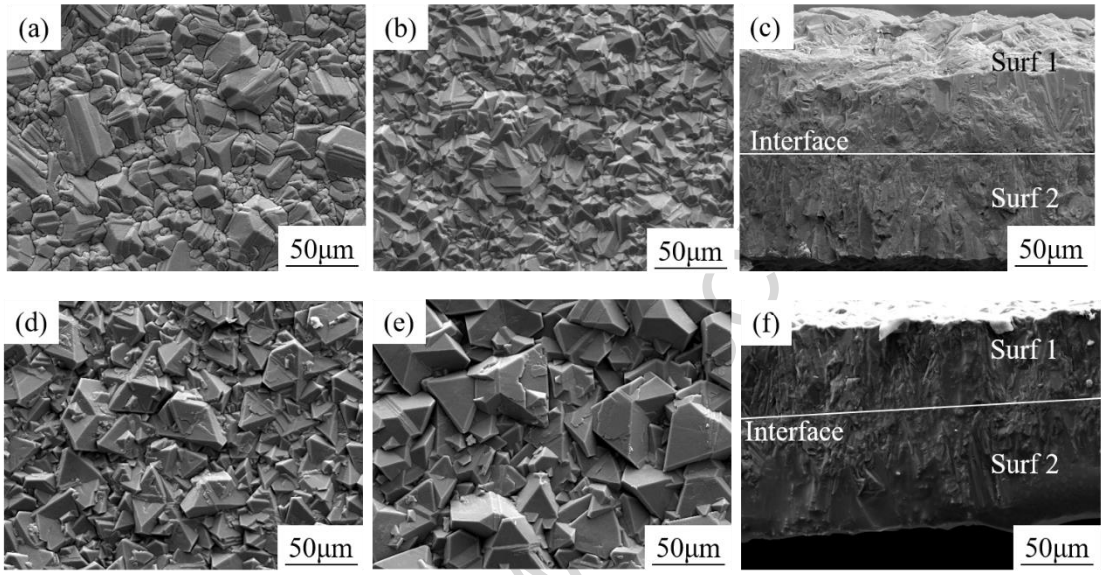

Fig. 1. SEM micrographs for sample #1: surface 1 (a), surface 2 (b), cross section (c); and sample #2: surface 1 (d), surface 2 (e), cross section (f).

3.2 Thickness uniformity

The thickness of the 2-inch diameter diamond films was measured from the center to the edge after the 1st and/or and 2nd growth run. To this aim the free-standing films were broken in two almost equal parts, and the cross section width has been measured using the optical microscope with accuracy of ±2 μm in different positions along the film diameter. This accuracy in the thickness measurement is close to the size of the symbols in Fig. 2, and, for this reason, is not shown on plots. The thickness radial profiles after the 1st and 2nd growth steps for sample #2 (Fig. 2) show a good uniformity (thickness deviation is as small as ~6% for both cases), thus the repeated growth did not cause a detrimental effect on the thickness uniformity.

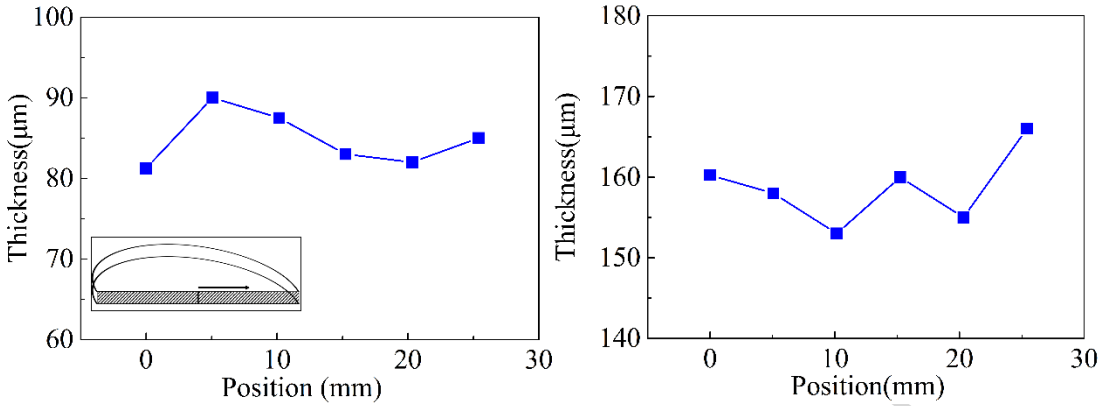

Fig. 2. Film thickness radial profiles for the single-layer sample #3 (left) and double-layer sample #2 (right). The position counts the distance from the sample center. Inset shows how the thickness was measured for the half-disks, the arrow indicating the direction from the diamond disk center towards to the edge.

3.3 XRD

XRD spectra for the sample #2 taken for angles (2θ) between 10° and 100° exhibits (111), (220) and (311) reflexes for both coarse-grain surfaces as displayed in Fig. 3. The diffraction pattern confirms the (111) dominant orientation of the crystallites, in agreement with the SEM observation (Fig. 1).

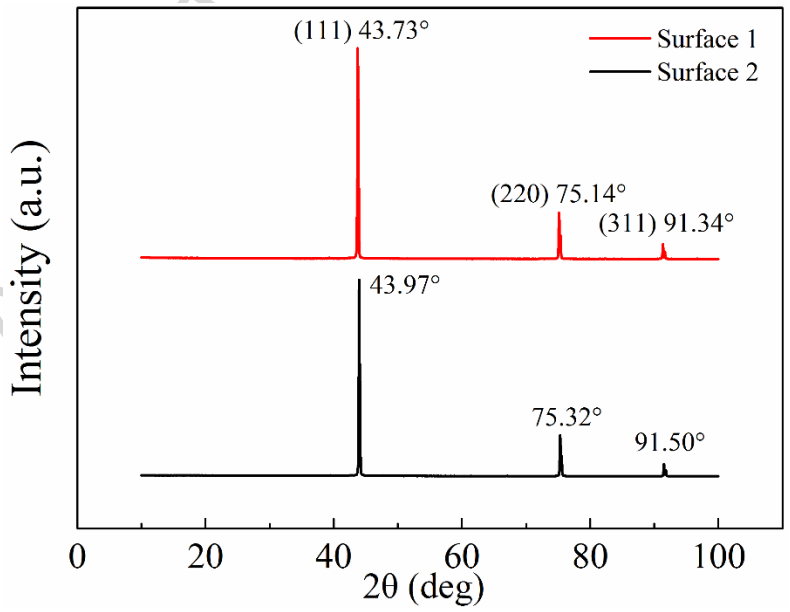

Fig. 3. XRD spectra for the surface 1 (top) and surface 2 (bottom) of the sample #2 demonstrate predominant (111) grain orientation on both film sides.

3.4 Raman spectroscopy

Raman spectra for all three samples, taken from both sides, are shown in Fig. 4. The spectra for both translucent samples #2 and #3 display the narrow strong diamond peak at 1332.5 cm^{-1}, without any signature of amorphous carbon contribution (Fig. 4a, b). The single layer #3 shows the diamond peak full width at half maximum (FWHM) $\Delta\nu$ as small as 2.3 $cm^{-1}$for growth side, which however increases to 4.0 $cm^{-1}$for nucleation side. In contrast, the bi-layered sample #2 demonstrates the diamond peak with small width values of 2.2 and 2.8 cm^{-1} for both sides (see also Table 1), this being in agreement with the fact that both analyzed surfaces were the growth sides with large grains, while more defective fine-grain nucleation layer was buried, and, therefore, was out of the probed volume upon the confocal Raman measurement.

The opaque sample #1 produced at enhanced concentration of methane 5%, has been measured by Raman spectroscopy on nucleation and growth sides *before* the repeated deposition, when that intermediate sample was a single layer. Its spectra display the significantly broaden diamond peak at 1332.5 cm^{-1}both for growth side ($\Delta\nu$ = 6.7 cm^{-1}) and nucleation side ($\Delta\nu$ = 9.5 cm^{-1}) (Fig. 4c). Moreover, a significant contribution of non-diamond sp2 carbon with prominent broad D-band at 1360 cm^{-1} and G-band at 1600 cm^{-1} is revealed on the nucleation side. A less, yet obvious, contamination of amorphous carbon is seen also on the opposite side, as deduced from the presence of a wide band centered at 1500 cm^{-1}. We concluded, therefore, that the opaque sample has a more defective structure compared to samples #2 and #3 as could be expected.

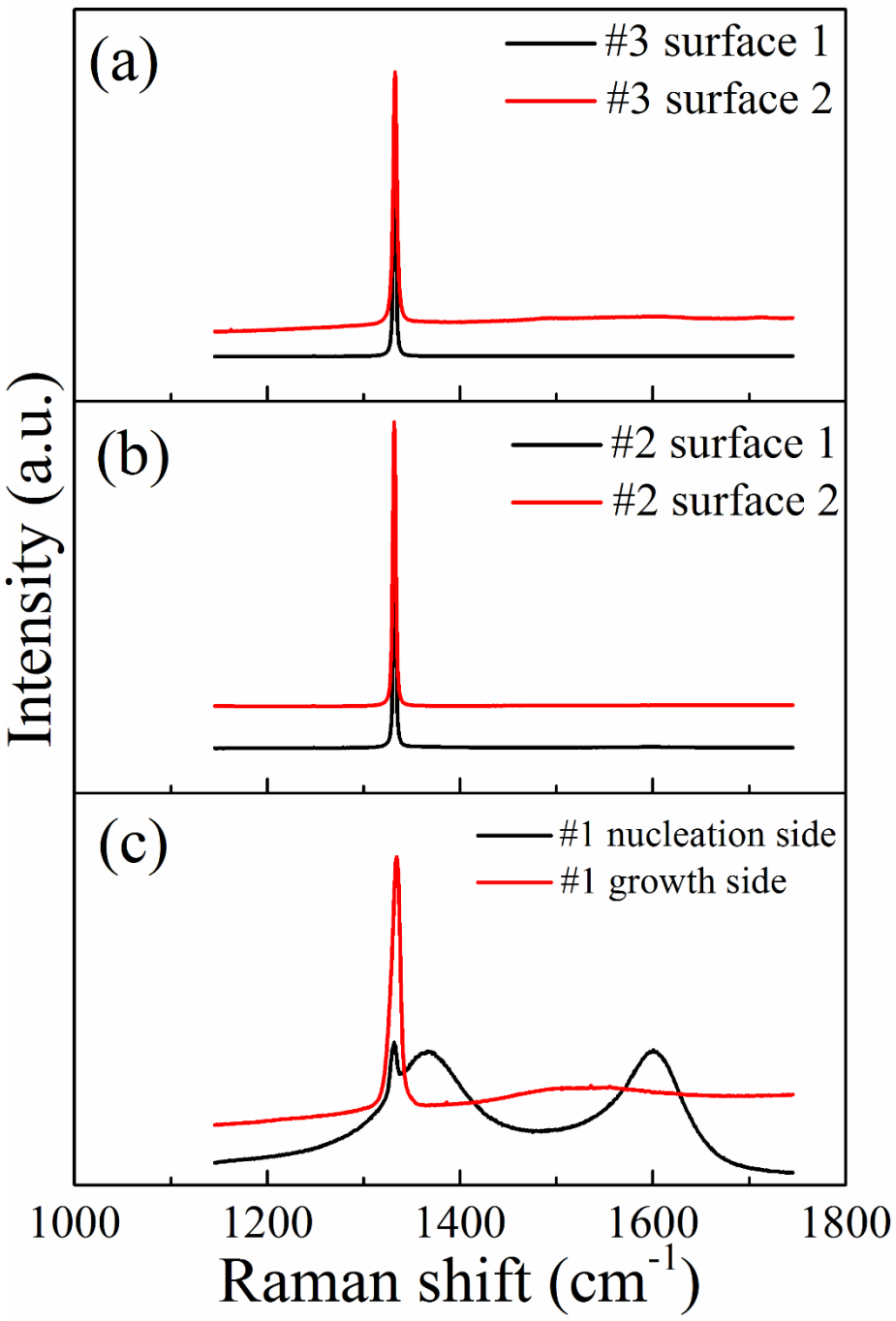

Fig. 4. Raman spectra for samples #3 (a), #2 (b) and #1 (c). The sample #1 has been measured before deposition of second layer.

3.5 Thermal conductivity

The temperature dependences of thermal conductivity *k*(T) for the three samples are shown in Fig. 5. All *k*(T) curves demonstrate as lightly increasing trend with temperature. The thermal conductivity for the opaque double-layer film (sample #1) is

a factor of 1.5 lower than the single-layer or double-layer translucent films #2 & 3. The k(T) values at room temperature are presented in Table 1. The TC inversely correlates with the Raman diamond peak width Δν (Table 1): the low k= 6.5 W/cm·K at room temperature was found for the opaque sample #1 with largest Δν, up to ≈10 cm^{-1}, whereas the double-layer sample #2 and the single-layer film #3 with a narrower Raman peak (2.2 ~ 4.0 cm^{-1}) revealed the higher (and similar) values k ≈ 9.5 W/cm·K. Thus, the doubling the film thickness by the growing the film on nucleation side does not give an increment in TC. This is reasonable result since the double-layer sample can be considered just as the material consisting of two identical parts with the same thermal properties.

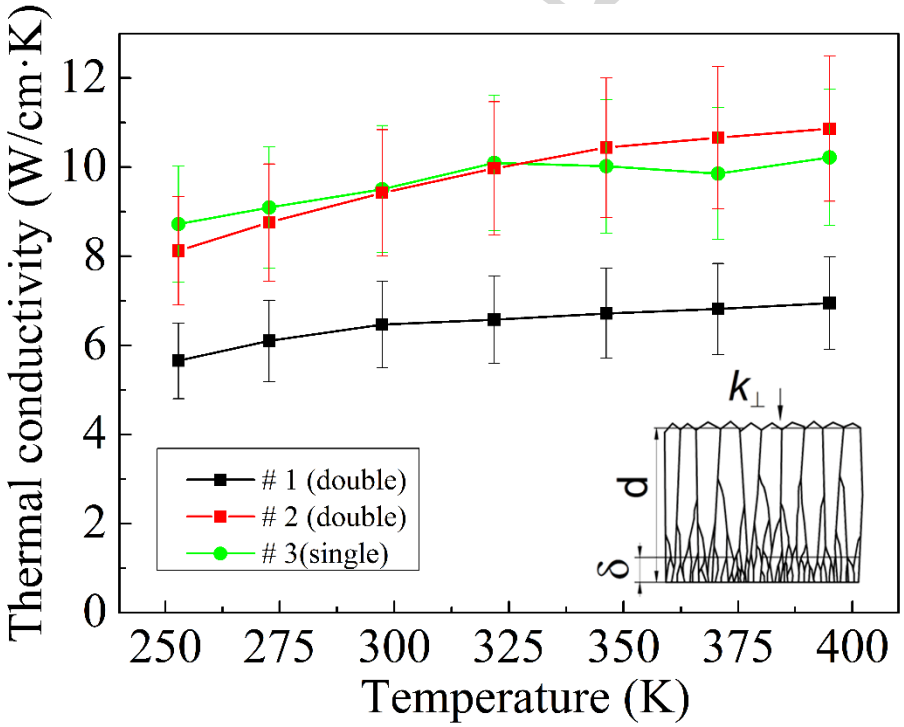

Fig. 5. The temperature dependences of thermal conductivity k(T) for the three samples measured by LFT: double-layer opaque film #1 (black squares); double-layer translucent film #2 (red squares), and single-layer translucent film (circles). Inset: schematics of the single-layer film with total thickness d containing a defective bottom part of thickness δ.

We observed the TC decrease towards low temperatures, while single crystals and

high quality coarse-grain diamond films are known to demonstrate the inverse trend [16,18,21-23]. The latter behavior is a consequence of different phonon scattering mechanisms superimposed on temperature dependent heat capacity of diamond *C*(T). The thermal conductivity can be estimated according to formula for phonon gas:

$$k = 1/3\ C\ \nu\ L \qquad (1)$$

where *L*(T) is phonon free path, and ν is sound speed (constant). The *k*(T) increases towards lower temperatures (between room temperature and the temperature for maximum *k*) because the phonon free path *L* increases due to reduction in phonon-phonon scattering frequency, which is the main source of thermal resistance at high temperatures. This improvement in *k*(T) occurs in spite of a decrease in heat capacity C(T) towards lower T. At very low T, typically below T≈100K, the phonon free path *L* varies only slightly, and the C(T) term in eq. (1) governs the temperature dependence, and *k*(T) rapidly decreases. The behavior of *k*(T) around maximum is controlled mainly by points defects. The contribution of different defects, grain boundaries and phonon scattering mechanisms to entire thermal resistance of diamond films was analyzed in detail, in particular, in [18,22]. However, the situation changes when the defects abundance becomes too high (or grain size reduces to submicron scale that restricts the value of *L* due to scattering by grain boundaries [11,24]). Typically, a monotonic decrease in *k*(T) upon cooling is observed for nanocrystalline films [24] and polycrystalline diamond films with room temperature TC of less than 1000 W/m·K [10,23]. Due to inhomogeneous columnar structure of the diamond films, and the presence of a fine-grained defective layer adjacent to nucleation side, the bottom part always has a lower TC compared to the top growth side, and exhibits a decrease in *k*(T) at *T* lower 400K [25]. In a simplest model with only two layers, “poor” nucleation layer and “good” coarse-grain top layer, the entire *k*(T) for the whole film will be determined by a superposition of the two different trends, the rising and falling ones. The schematic structure of the film in cross-section, with the two layers of different quality, is displayed in inset in Fig. 5. We estimated *k*(T) for the bi-layer model using the total thermal resistance as the sum of the partial

resistances for each layer:

$$k_{total} = (\delta_1+\delta_2)/(\delta_1/k_1+\delta_2/k_2) \qquad (2)$$

where δ_1, k_1 and δ_2, k_2 are thickness and thermal conductivity of the bottom and top layers, respectively. As an example, a double-growth sample was considered with thickness of 170 μm consisting of 50 μm thick nucleation layer with low k_1 = 5.0 W/cm·K, at which the k(T) should falling rather than rising trend towards low temperatures, and the rest 120 μm thick coarse-grain top layer. It was found that to get the experimentally observed value of k_{total}= 9.5 W/cm·K, the top layer should have the TC as high as 14.9 W/cm·K, with expected rising trend [10,23,26]. In our case the impact of the low-k nucleation layer seems to be somewhat stronger than that of higher-k of the top layer, and we observe a slight decrease in k(T) toward low T for the temperature range of 250 – 400K, for translucent and opaque films (Fig. 5). The single layer (sample #3) and bi-layer (sample #2) produced in identical growth conditions exhibit identical TC, as follows from eq. (2) and because the doubling the thickness is simply a summation of two identical 80 thick μm single layer parts (possibly with a complex interior) with the same TC, that does not change the total TC value.

Note that the perpendicular TC as measured by laser flash technique is more sensitive to the presence of a fine-grained defective layer adjacent to nucleation side compared to in-plane TC. Qualitatively, it is clear why LFT method is so sensitive to bottom layer, even if it is relatively thin. For low enough k_1 the overall TC will follow the k(T) for this poor quality portion of the film, while in case of in-plane TC this part will be simply excluded from the heat transport, and the loss in TC is simply proportional to this layer thickness.

Conclusions

Free-standing 160 μm-thick polycrystalline diamond film with two growth sides (with the nucleation side in middle) have been produced by MPCVD to obtain a similar grain size on both surfaces. Both the primary single-layer film and the

double-layer film with the thickness increased by two times, showed good thickness uniformity. The temperature dependence of perpendicular thermal conductivity k(T) for the translucent samples was measured by laser flash technique and gave the same thermal conductivity of 9.5±1.4 W/cm·K at room temperature for the single-layer and the double-layer films grown at almost identical process parameters. A slight decrease in k(T) toward low T for the temperature range of 250 – 400K was observed and ascribed to the effect of poor quality material adjacent to nucleation side.

Acknowledgements

The financial supports from the National Science Fund for Distinguished Young Scholars (Grant No. 51625201), the National Natural Science Foundation of China (Grant No. 51372053), Innovative Research Groups of the National Natural Science Foundation of China (Grant No. 11421091), and International Science & Technology Cooperation Program of China (2015DFR50300) are highly appreciated.

Prime novelty statement

We firstly fabricated double-side coarse-grain freestanding polycrystalline diamond with microwave plasma chemical vapor deposition (MPCVD) by a repeated diamond growth on nucleation side of a primary free-standing film. The thermal conductivity of double-layer and single-layer diamond films was found to be identical (9.5±1.4 W/cm·K at room temperature) as measured by a laser flash technique.

References

[1] R.S. Balmer, J.R. Brandon, C.L. Clewes, H.K. Dhillon, J.M. Dodson, I. Friel, P.N. Inglis, T.D. Madgwick, M.L. Markham, T.P. Mollart, N. Perkins, G.A. Scarsbrook, D.J. Twitchen, A.J. Whitehead, J.J. Wilman, S.M. Woollard, Chemical vapour deposition synthetic diamond: materials, technology and applications, J. Phys.: Condens. Matter 21 (2009) 364221.

[2] J. E. Graebner, S. Jin, G.W. Kammlott, J.A. Herb, C.F. Gardinier, Unusually high thermal conductivity in diamond films, Appl. Phys. Lett. 60 (1992) 1576-1578.

[3] C. Zweben, Revolutionary new thermal management materials. Electronics Cooling, 11 (2005) 36-37.

[4] P.W. May, H.Y. Tsai, W.N. Wang, J.A. Smith, Deposition of CVD diamond onto GaN, Diam. Relat. Mater. 15 (2006) 526-530.

[5] H. Sun, R.B. Simon, J.W. Pomeroy, D. Francis, F. Faili, D.J. Twitchen, M. Kuball, Reducing GaN-on-diamond interfacial thermal resistance for high power transistor applications, Appl. Phys. Lett. 11(2015) 111906.

[6] S. Piehler, T. Dietrich, M. Rumpel, T. Graf, M.A. Ahmed, Highly efficient 400 W near-fundamental-mode green thin-disk laser, Optics Lett. 41(2016) 171-174.

[7] S. Gloor, W. Luthy, H.P. Weber S.M. Pimenov, V.G. Ralchenko, V.I. Konov, A.V. Khomich, UV laser polishing of thick diamond films for IR windows. Appl. Surf. Sci. 138-139 (1999) 135-139.

[8] E. Anoikin, A. Muhr, A. Bennett, D. Twitchen, H. de Wit, Diamond optical components for high-power and high-energy laser applications. In *SPIE LASE*, pp. 93460T-93460T. International Society for Optics and Photonics (2015).

[9] C. Wild, R. Koidl, N. Herres, W. Mueller-Sebert, H. Walcher, R. Kohl, N. Herres, R. Locher, R Samlenski, R. Brenn, Chemical vapor deposition and characterization of smooth {100}-faceted diamond films, Diam. Relat. Mater. 2 (1994) 158-168.

[10] J.E. Graebner, S. Jin, J.A. Herb, C.F. Gardinier, Local thermal conductivity in chemical vapour deposited diamond, J. Appl. Phys. 76 (1994) 1552-1556.

[11] J.Anaya, S.Rossi, M.Alomari, E.Kohn, L.Tóth, B.Pécz, K.D.Hobart, T.J.Anderson, T.I.Feygelson, B.B.Pate, M.Kuball, Control of the in-plane thermal conductivity of ultra-thin nanocrystalline diamond films through the grain and grain boundary properties, Acta Mater. 103 (2016) 141–152.

[12] R.B.Simon, J. Anaya, F. Faili, R.Balmer, G.T.Williams, D.J. Twitchen, M. Kuball. Effect of grain size of polycrystalline diamond on its heat spreading properties, Appl. Phys. Express, 6 (2016) 061302.

[13] A.V. Sukhadolau, E.V. Ivakin, V.G. Ralchenko, A.V. Khomich, A.V. Vlasov, A.F. Popovich, Thermal conductivity of CVD diamond at elevated temperatures, Diam. Relat. Mater. 14 (2005) 589-593.

[14] J. E. Graebner, S. Jin, G.W. Kammlott, B. Bacon, L. Seibles, W.Banholzer, Anisotropic thermal conductivity in chemical vapor deposition diamond, J. Appl. Phys, 71 (1992) 5353–5356.

[15] S.Coe, R.Sussmann, Optical, thermal and mechanical properties of CVD diamond, Diam. Relat. Mater. 9 (2000) 1726–1729.

[16] A.V. Inyushkin, A.N. Taldenkov, V.G. Ralchenko, I.I. Vlasov, V.I. Konov, A.V. Khomich, R.A. Khmelnitskii, A.S. Trushin, Thermal conductivity of polycrystalline CVD diamond: effect of annealing-induced transformations of defects and grain boundaries, Phys. Stat. Sol. (a), 205 (2008) 2226–2232.

[17] A. Vlasov, V. Ralchenko, S. Gordeev, D. Zakharov, I. Vlasov, P. Belobrov, Thermal properties of diamond/carbon composites, Diam. Relat. Mater. 9 (2000) 1104-1109.

[18] A.P. Bolshakov, V.G. Ralchenko, V.Y. Yurov, A.F. Popovich, I.A. Antonova, A.A. Khomich, E.E. Ashkinazi, S.G. Ryzhkov, A.V. Vlasov, A.V. Khomich, High rate growth of single crystal diamond in microwave plasma in H_2-CH_4 and H_2-CH_4-Ar mixtures in presence of intensive soot formation, Diam. Relat. Mater, 62 (2016) 49-57.

[19] J.E. Graebner, Thermal conductivity of CVD diamond films: Techniques and results, Diamond Films and Technol, 3 (1993) MYU, Tokyo.

[20] V.I. Nepsha, Heat capacity, conductivity and the thermal coefficient of

expansion, in Handbook of Industrial Diamonds and Diamond Films, ed. by M. A. Prelas et al. N.Y., Marcel Dekker, 1997, pp.147-192.

[21] C.J.H. Wort, C.G. Sweeney, M.A. Cooper, G.A. Scarsbrook, R.S. Sussman, Thermal properties of bulk polycrystalline CVD diamond, Diam. Relat. Mater. 3 (1994) 1158-1167.

[22] J.E. Graebner, M.E. Reiss, L. Seibles, T.M. Hartnett, R.P. Miller, C.J. Robinson, Phonon scattering in chemical-vapor-deposited diamond, Phys. Rev. B 50 (1994) 3702-3713.

[23] E. Worner, E. Pleuler, C. Wild, P. Koidl, Thermal and optical properties of high purity CVD-diamond discs doped with boron and nitrogen, Diam. Relat. Mater. 12 (2003) 744-748.

[24] M. Shamsa, S. Ghosh, I. Calizo, V. Ralchenko, A. Popovich, A.A. Balandin, Thermal conductivity of the nitrogen doped nanocrystalline diamond films on silicon, J. Appl. Phys. 103 (2008) 083538.

[25] J. Anaya, H. Sun, J. Pomeroy, M. Kuball, Thermal management of GaN-on-diamond high electron mobility transistors: Effect of the nanostructure in the diamond near nucleation region. In Thermal and Thermomechanical Phenomena in Electronic Systems (ITherm), 15th IEEE Intersociety Conf., May 31, 2016, pp. 1558-1565.

[26] A.V. Sukhadolau, E.V. Ivakin, V.G. Ralchenko, A.V. Khomich, A.V. Vlasov, A.F. Popovich, Thermal conductivity of CVD diamond at elevated temperatures, Diam. Relat. Mater. 14 (2005) 589-593.

Figure captions

Fig. 1. SEM micrographs for sample #1: surface 1 (a), surface 2 (b), cross section (c); and sample #2: surface 1 (d), surface 2 (e), cross section (f).

Fig. 2. Film thickness radial profiles for the single-layer sample #3 (left) and double-layer sample #2 (right). The position counts the distance from the sample center. Inset shows how the thickness was measured for the half-disks, the arrow indicating the direction from the diamond disk center towards to the edge.

Fig. 3. XRD spectra for the surface 1 (top) and surface 2 (bottom) of the sample #2 demonstrate predominant (111) grain orientation on both film sides.

Fig. 4. Raman spectra for samples #3 (a), #2 (b) and #1 (c). The sample #1 has been measured before deposition of second layer.

Fig. 5. The temperature dependences of thermal conductivity k(T) for the three samples measured by LFT: double-layer opaque film #1 (black squares); double-layer translucent film #2 (red squares), and single-layer translucent film (circles). Inset: schematics of the single-layer film with total thickness d containing a defective bottom part of thickness δ.

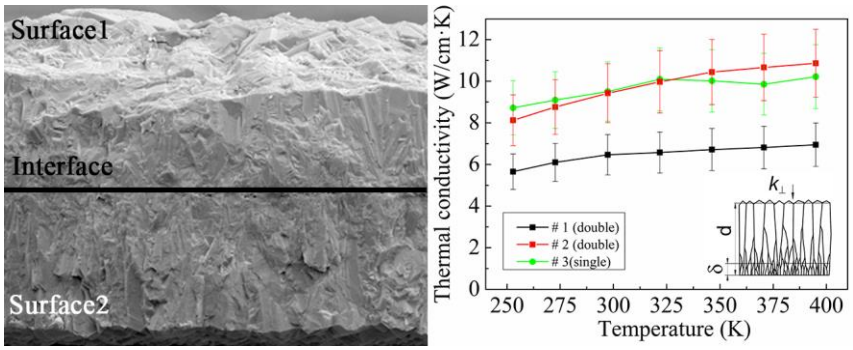

Graphical abstract